

Evolution of Microstructure and Residual Stress in Hot Rolled Ti-6Al-4V Plates Subjected to Different Heat Treatment Conditions

William Rae^{1,2,a,*}, Salah Rahimi^{2,b}

¹Design, Manufacture & Engineering Management (DMEM) Department, University of Strathclyde, 75 Montrose Street, Glasgow, UK

²Advanced Forming Research Centre (AFRC), University of Strathclyde, 85 Inchinnan Drive, Glasgow, UK

^awilliam.rae@strath.ac.uk, ^bsalah.rahimi@strath.ac.uk

Keywords: Contour Method, X-Ray Diffraction, Titanium Alloy, Phase Transformation

Abstract. Hot rolled Ti-6Al-4V plate samples were taken from three different stages of an industrial heat treatment process; one as-rolled and two heat treated. This was followed by microstructure characterization using optical microscopy. Surface and through-thickness residual stress was determined using a combination of X-ray diffraction (XRD) and the contour method. Measured residual stress distributions showed similarities in distribution with that obtained for rolled Al-7050 alloy; including compressive troughs near the outer thickness on both sides, leading towards a tensile zone around the center with a local minima at the plate center thickness. Microstructure and residual stress data was then used to draw comparisons between the investigated conditions.

Introduction

Titanium alloys are often selected as critical components in the aerospace sector due to their exceptionally high strength-to-weight ratio and ability to produce different microstructures, with tailored mechanical properties, by thermo-mechanical processing at elevated temperatures. Thermo-mechanical processing may generate residual stress which can lead to distortion out of dimensional tolerance during subsequent manufacturing processes; such as during machining [1], and can also affect material performance in service; such as reducing fatigue life [1]. The difficulty arises because Ti alloys usually have a complex, multi-phase microstructure, which varies within a component depending on process history [1]. This makes the final residual stress distribution highly dependent on microstructure and deformation history. Residual stress arises from heterogeneity in plastic deformation and during thermo-mechanical processing, phase transformation, and the differential gradient between colder outer surface and hot inner interior induced during cooling. The latter would be even more intensified by non-uniform heat exchange with the cooling environment. The deformation in Ti alloys is complex due to the inherent thermal and mechanical anisotropy of the constituent phases. Furthermore, in the temperature range of interest (600°C – 950°C), the material undergoes a reversible α - β phase transformation, which can contribute to stress relaxation [2].

Thus, it is imperative that the evolution of residual stress is understood when designing and modifying microstructure for high value, critical aerospace components. The aim of this work was to evaluate microstructure and the through-thickness residual stress distribution induced by thermo-mechanical and subsequent industrial heat treatment processing of 38 mm Ti-6Al-4V plate, using multiple residual stress measurement techniques.



Materials & Methods

Materials & Processing. The material selected for this study was Ti-6Al-4V in the form of a 38 mm thickness rolled plate with dimensions of approximately $38 \times 250 \times 250 \text{ mm}^3$; these sections were removed from industrially processed plates with a width of 1000 mm^3 by means of flame cutting. The nominal chemical composition of the alloy is provided in Table 1. Three plate conditions were investigated: one as-rolled (AR) condition which was deformed at approximately 950°C , and two conditions which were subjected to varying subsequent post-rolling annealing treatments (HT1 and HT2) high in the $\alpha+\beta$ phase field ($>900^\circ\text{C}$) followed by air cooling. Both surfaces of HT2 were also subjected to shot blasting and its influence on residual stress was of interest. It was noted that the use of flame cutting would affect the overall residual stress distribution in the samples, however as this was carried out for all plate conditions it was deemed that the gathered data would allow for adequate comparison, and the original plate residual stress could be ascertained by further modelling which was out-with the scope of this work.

Table 1. Nominal chemical composition for Ti-6Al-4V alloy used in study (wt%).

V	Fe	Al	O	C	N	Ti
4	0.25	6	0.13	0.08	0.03	Bal.

Microstructure Characterization. Light microscopy was utilized to gain an understanding of the grain morphology and microstructural evolution in the materials. Three 10 mm^3 cubes were cut from each plate condition at a distance of over $\sim 25 \text{ mm}$ from the plate edge to minimize the chance of the microstructure being effected by the flame cut. Metallographic preparation was conducted until a mirror finish was achieved, followed by chemical etching using Kroll's Reagent (2% HF, 6% HNO_3 , and 92% H_2O) to reveal the microstructure. A Leica DM12000M Optical Microscope was then used to acquire micrographs at a range of magnifications.

Residual Stress Measurement. Residual stress analysis was carried out on each plate using a combination of X-ray Diffraction (XRD) for surface measurements, and the contour method for through-thickness measurements; providing complementary data [3]. As it has previously been shown that the residual stress distribution parallel to the rolling direction is largely uniform [4], it was desired to investigate the residual stress distribution perpendicular to the rolling direction, along the center of the plate. The out-of-plane residual stress, σ_{zz} , was measured using both techniques.

Firstly, non-destructive XRD was carried out using a PROTO LXR X-ray diffractometer system and the $\sin^2\psi$ method. The diffraction peak at a Bragg angle of 140° , corresponding to the $\{211\}$ crystallographic plane in the α phase, was used to calculate residual strain which was then converted to residual stress, assuming a Young's Modulus of 118 GPa and Poisson's Ratio of 0.342. Although Ti-6Al-4V is a dual phase alloy, it consists of approximately 92% α phase at room temperature and therefore the stress associated with the β phase is assumed to have a minimal effect on the overall residual stress magnitude [2]. Nine measurements were performed on the top surface of each plate at increments of 25 mm from the plate center position, with three measurements along the base at increments of 50 mm from the center. Nine ψ -offset angles in the range of $\pm 30^\circ$ were employed.

A 2-D map of out-of-plane residual stress perpendicular to the rolling direction was produced using the contour method. The plates were cut through the center by electrical discharge machining (EDM) using a 250 μm brass wire. The outline and surface topography of the cut surfaces were then measured by means of a Mitutoyo Crysta Apex C coordinate measuring machine (CMM). Co-ordinate data was obtained at increments of 0.4 mm through the thickness and 1 mm along the length of the surface. The measured data was then cleaned to minimize

outliers, followed by alignment of the two corresponding surface datasets to one coordinate system, which was then linearly interpolated onto a common grid and averaged to form one set of data for each plate condition. A bivariate cubic spline was fit to the data with knot spacing of 10 mm and 5.6 mm in the x (width) and y (thickness) direction, respectively. A 3-D finite element (FE) model was produced from this fitted data and the original residual stresses were computed by forcing the surface into the reverse shape of the averaged topography data.

Results & Discussion

Microstructure Characterization. The multi-orientation light micrographs obtained for each plate condition are presented in Fig. 1. The AR condition exhibited a high fraction of elongated α lamellae along the rolling direction with some globular α in a fine transformed β matrix. The HT1 condition shows a clear break-up of α lamellae in the transverse and normal planes with an increased fraction of more equiaxed, globular α with Widmanstätten α tending to replace the fine α_s observed in the AR condition. The HT2 condition shows a greater degree of α_p fragmentation than HT1, with less Widmanstätten α and an accompanying increase in fraction and size of globularised grains; however, a large amount of elongated α lamellae still remain.

The break-up of α lamellae by globularization as observed in the HT1 and HT2 conditions was characteristic of recrystallization annealing high in the $\alpha+\beta$ phase field ($>900^\circ\text{C}$) [5]. An increased fraction and size of globular α in the HT2 condition may be due to a further annealing cycle; or increased temperature or duration than that experienced in the HT1 condition, resulting in the progression of globularization kinetics [5]. Globularization in Ti-6Al-4V has been associated with stress relaxation; due to rearrangement of dislocations which can annihilate as they move through the lattice, reducing dislocation density and therefore internal strain [6]. Thus, it was thought that the microstructural evolution observed may be indicative of stress relaxation.

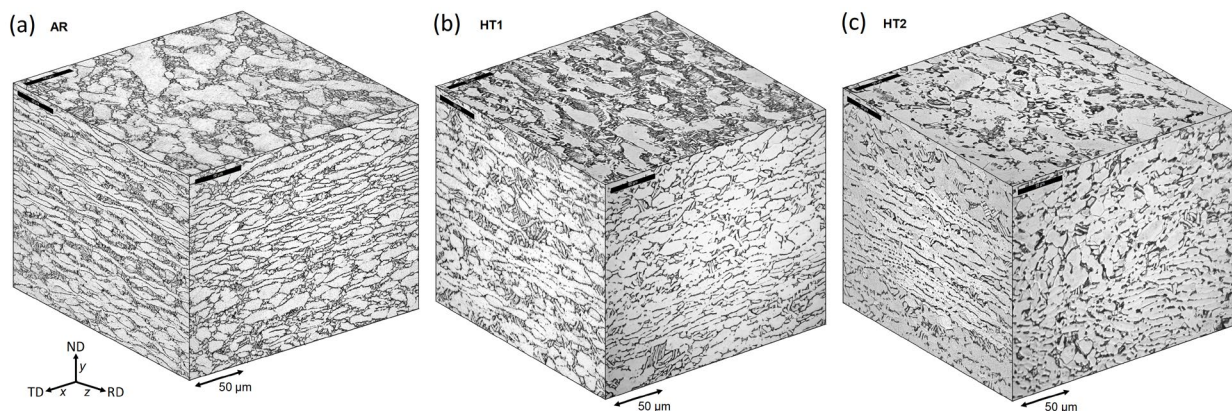


Figure 1. Multi-orientation light microscope images of (a) AR; (b) HT1; and (c) HT2 conditions.

Residual Stress Measurement. The surface residual stress measurements obtained by XRD are presented in Fig. 2 for all conditions. The AR plate exhibited a low magnitude of tensile surface residual stress for all measurement points, with a peak stress of +69 MPa on the top surface at a distance of 25 mm from the plate center. Measured stresses reduced towards +18 MPa outwards from this point. The stress distribution on the bottom was lower and ranged from +7 MPa to +25 MPa. The HT1 condition contained similar magnitudes of residual stress, however this was largely uniform along the top surface with an average of +45 MPa. The bottom surface exhibited a compressive stress of -34 MPa at -50 mm from the plate center with the other two points showing low tensile values of between 0 and +20 MPa. On the other hand, the HT2 condition exhibited much higher magnitudes of compressive residual stress for all measured points. This was largely uniform along both surfaces with an average value of approximately -300 MPa and -500 MPa for the top and bottom, respectively. The similarities in magnitudes between the AR

and HT1 conditions suggest that comparable cooling conditions may have been used for both processes. The highly compressive residual stresses measured in the HT2 condition is likely to be due to shot-blasting which was applied to both sides of the material after heat treatment.

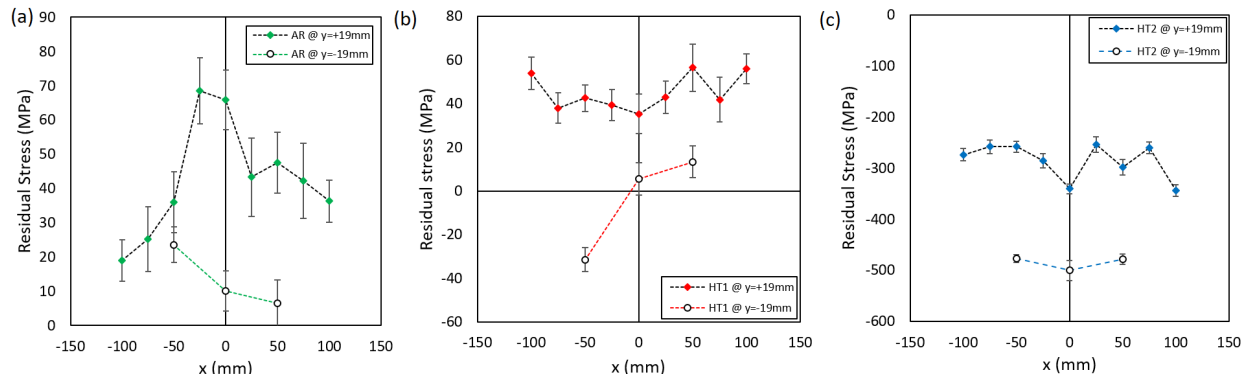


Figure 2. Surface residual stress distribution as determined by XRD for (a) AR; (b) HT1; and (c) HT2.

The contour method residual stress results for the AR condition (Fig. 3a) show a clear compressive trough on either side of the plate within the first 10 mm thickness. This region had a peak compressive residual stress of -100 MPa and is shown to elongate along the x-direction. A balancing tensile region was then observed over the following 5-10 mm on both sides with a local minima region noted at approximately the center of the plate thickness. A maximum tensile stress of +58 MPa was noted. This trend is further exemplified in the combined contour and XRD through-thickness line profiles presented in Fig. 4a; where the contour method results show good agreement with the surface data provided by XRD. On comparison with the through-thickness residual stress distribution obtained by Prime and Hill for cold-rolled aluminum (Fig. 4b), numerous similarities can be noted [4]. Both data show compressive troughs in within 20% of the outer surface followed by balancing tensile regions and a local minima at approximately 50% of the plate thickness. This particular residual stress distribution is thus likely to be primarily due to heterogeneous plastic deformation during rolling as it has been observed in both hot and cold-rolled plates.

On evaluation of the HT1 contour data (Fig. 3b and 4c), a similar trend is noted including the compressive troughs and local minima around $y = 0$ mm, however the magnitudes of residual stress in the compressive regions are much higher than that of the AR condition. This is particularly visible in the top region between $x = -50$ and $+50$ mm. The maximum compressive stress was observed in this region with a magnitude of -220 MPa, with a comparatively lower local maximum compressive stress on the bottom side of -120 MPa. As the residual stress distribution continued to somewhat resemble that of the AR condition it is thought that this indicates the heat treatment did not lead to full relaxation of residual stress. Additionally, the increased magnitudes in the top compressive region suggests that an aspect of post rolling treatment induced increased residual stress near the top surface. On examination of the contour results for the HT2 condition (Fig. 3c and 4d), the increased intensity of the compressive trough near the top surface is immediately apparent, stretching over 200 mm in the x-direction. The maximum compressive stress in this region was noted to be -220 MPa, as with HT1, with a maximum on the bottom side of -100 MPa. The characteristic rolled plate residual stress distribution can be seen for HT2 but is less prominent than the AR or HT1 condition.

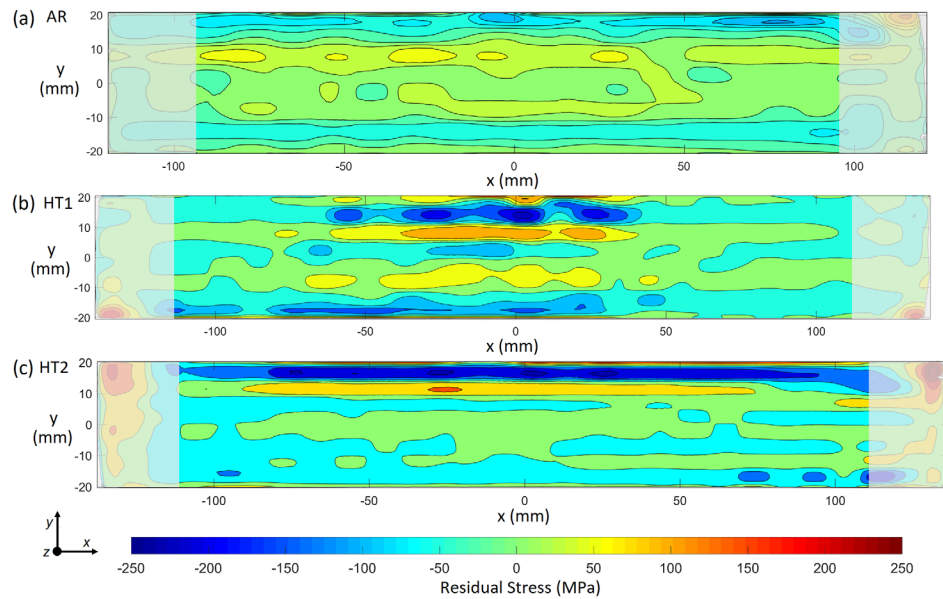


Figure 3. 2-D out-of-plane residual stress maps of samples as determined by the contour method for (a) AR, (b) HT1 and (c) HT2 plate conditions. The outer 25 mm of each plate has been shaded in grey as it was affected by the flame cut and therefore not considered in analysis.

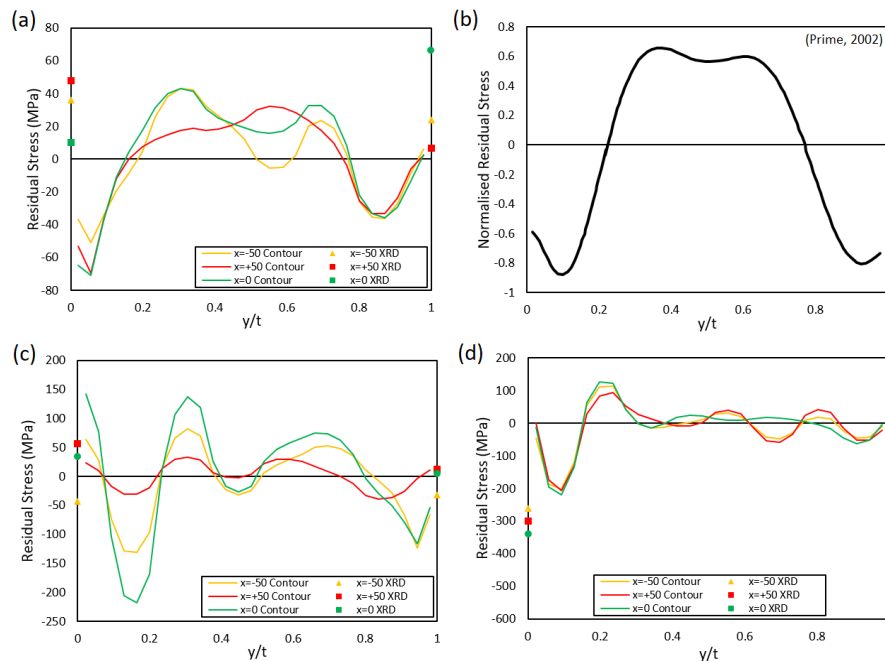


Figure 4. Combined XRD and through-thickness contour method residual stress line profile at $x = -50$ mm, $x = 0$ mm and $x = +50$ mm for (a) AR; (c) HT1; and (d) HT2 conditions. Normalized through-thickness residual stress line profile of cold-rolled 7050-T74 plate provided in (b) for comparison (adapted from [4]). Y-axis has been normalized for all figures.

The further decreased prominence of the rolled plate distribution in HT2, especially for y/t above 0.3, suggests that heat treatment may have relaxed initial rolling induced residual stress by a greater extent than in HT1 condition. This was likely due to either increased annealing temperature or soak duration and is supported by the observation of increased break-up of α lamellae in the HT2 microstructure.

The compressive troughs near the bottom surface of all conditions were found to be of similar magnitude (-50 to -100 MPa), whereas the troughs near the top surface showed a much increased

magnitude for the HT1 and HT2 condition. Increased magnitudes of compressive near-surface residual stress are commonly associated with higher thermal gradients in the region [3]. This indicates that the top surfaces of the HT1 and HT2 conditions were likely exposed to higher cooling rates compared to the AR condition. The consistency of the residual stress distribution of the bottom surfaces suggests slower cooling rates in this area for all conditions; likely through conductive cooling, indicating that the bottom surface was not exposed to the air. This suggests that although annealing acts to relieve original residual stresses and provide a more homogeneous microstructure, the final residual stress distribution is highly dependent on post-heat treatment cooling rates [5]. Further work should be completed to quantify the effect of cooling rate on the residual stress distributions using the inverse heat transfer coefficient method.

Conclusions

- All hot-rolled plate conditions showed similarities with the residual stress distribution for cold-rolled Al plate reported in literature, indicating that the plastically induced residual stress from rolling is not fully relieved by processing at elevated temperature.
- Heat treated conditions showed a clear break-up of α lamellae but this is not thought to have greatly affected the residual stress magnitudes or distribution.
- Increased cooling rates may have caused increased compressive residual stress near the top surface of the heat treated conditions.

Acknowledgements

This work was supported by the Scottish Association for Metals (SAM) and Engineering and Physical Sciences Research Council (EPSRC) grant (EP/1015698/1). The authors would like to thank TIMET for the provision of materials, and also Aubert & Duval for their support on the project. The research was performed at the Advanced Forming Research Centre (AFRC), which receives partial financial support from the UK's High Value Manufacturing Catapult.

References

- [1] M. G. Glavicic, D. U. Furrer, and G. Shen, "A Rolls-Royce Corporation industrial perspective of titanium process modelling and optimization: current capabilities and future needs," *J. Strain Anal. Eng.*, vol. 45, no. 5, 2010, pp. 329-335. <https://doi.org/10.1243/03093247JSA577>
- [2] E. Alabort, P. Kontis, D. Barba, K. Dragnevski, and R. C. Reed, "On the mechanisms of superplasticity in Ti-6Al-4V," *Acta Mater.*, vol. 105, 2016, pp. 449-463. <https://doi.org/10.1016/j.actamat.2015.12.003>
- [3] Rae, W., Lomas, Z., Jackson, M., & Rahimi, S., "Measurements of residual stress and microstructural evolution in electron beam welded Ti-6Al-4V using multiple techniques," *Mat. Char.*, vol. 132, 2017, pp. 10-19. <https://doi.org/10.1016/j.matchar.2017.07.042>
- [4] Prime, M.B. and Hill, M.R., "Residual stress, stress relief, and inhomogeneity in aluminum plate". *Scripta Materialia*, 2002, vol. 46, no. 1, pp.77-82. [https://doi.org/10.1016/S1359-6462\(01\)01201-5](https://doi.org/10.1016/S1359-6462(01)01201-5)
- [5] Stefansson, N., and S. L. Semiatin. "Mechanisms of globularization of Ti-6Al-4V during static heat treatment," *Metall. Mat. Trans. A*, 2003, vol. 34, no.3, pp. 691-698. <https://doi.org/10.1007/s11661-003-0103-3>
- [6] Babu, B., & Lindgren, L. E., "Dislocation density based model for plastic deformation and globularization of Ti-6Al-4V". *Int. J. Plasticity*, 2013, 50, pp. 94-108. <https://doi.org/10.1016/j.ijplas.2013.04.003>